Probing low-temperature water ice phases using electron-stimulated desorption

M.T. Sieger, T.M. Orlando *

W.R. Wiley, Environmental Molecular Sciences Laboratory, Pacific Northwest National Laboratory, MS K8-88, PO Box 999, Richland, WA 99352, USA

Abstract

Low-energy electron-stimulated desorption (ESD) of D^+ from D_2O has been used to examine the phase and growth behavior of nanoscale vapor-deposited ice films grown on Pt(111) between 90–155 K. The D^+ yield from porous amorphous solid water (deposited at 90 K) shows evidence for sintering near 120 K, increases between 120 and 140 K, and then drops at the amorphous–crystalline phase transition near 155 K. Ice deposited at 155 K forms an epitaxial crystalline film, with a D^+ yield nearly one-third larger than the yield from crystalline films prepared by annealing the amorphous phase. This suggests that the film formed by annealing may have a different crystalline ordering or morphology than the epitaxial film deposited between 150 and 155 K. Ice deposited at 90 K on top of the epitaxial film is amorphous, but it crystallizes to a form similar to that of the underlying crystalline ice substrate. This suggests that, in this case, the buried two-dimensional interface nucleates the crystallization. © 2000 Elsevier Science B.V. All rights reserved.

1. Introduction

There has been a recent resurgence of interest in the growth morphology and crystallization kinetics of nanoscale ice films grown in ultrahigh vacuum (UHV). An understanding of low-temperature ice is desirable not only from a purely fundamental standpoint, but it is also important for studies of icy bodies in planetary and interstellar space [1]. Recent studies by Sack and Baragiola [2], Smith and co-workers [3,4], Speedy et al. [5], and Löfgren et al. [6] have examined the crystallization kinetics of thin amorphous solid water films by temperature programmed desorption (TPD).

Other experiments have focused on the film morphology and density under various growth conditions [7,8].

Of the many known phases of ice, only three play an important role in the temperature and pressure environment of UHV: porous amorphous solid water (P-ASW), amorphous solid water (ASW), and crystalline ice (CI). Each of these phases is easily prepared by controlling the deposition temperature and annealing history. Water deposited on substrates at temperatures below 130 K tends to form ASW, with local bonding that may be similar to that of liquid water [9]. Below 100 K, P-ASW is formed [7,8,10,11], which is characterized by a high surface area and low density. Annealing P-ASW to 120 K collapses the pores, generating normal ASW. ASW is a meta-

* Corresponding author. Fax +1-509-376-6066.
E-mail address: tm_orlando@pnl.gov (T.M. Orlando)

stable state of ice, and crystallizes rapidly near 155 K to form a polycrystalline ice (PCI) film [2–5,10,11]. If the substrate has a good lattice match to crystalline ice, deposition above 140 K (or very slow deposition at lower temperatures) leads to an oriented epitaxial crystalline ice (ECI) film [12–14]. Growth of this film is thought to proceed according to the Stranski–Krastanov mechanism, in which the formation of the bilayer is followed by the creation of large domains of three-dimensional ice [15].

In our earlier work [16,17], the electron-stimulated desorption (ESD) of D^+ from ASW, P-ASW, and CI D_2O films was shown to exhibit differences in the total yield and ion velocity distributions as a function of ice temperature. Since ESD is a surface-sensitive probe, the different behaviors can be due to different surface structures, morphologies and defect densities. The excitations responsible for cation emission have been assigned to localized two-hole and two-hole–one-electron ionic configurations [18]. Recent evidence suggests that these dissociative excitations, and others leading to D^- emission, are sensitive to the local hydrogen-bonding environment of the water molecule [16,17,19,20]. The roughness of the surface also appears to affect the ion escape probability [17]. Although our surface-sensitive ESD measurements can infer only the state of the surface layer of our samples, the fact that the D^+ yields from the different phases are different allows us to observe phase transitions and growth dynamics using ESD.

In this paper, we report measurements utilizing ESD to probe transitions in the surface of nanoscale [40 ML (monolayer)] ice films as a function of temperature. Crystallization of ASW–Pt(111) forms a PCI film that is characterized by a D^+ yield nearly a factor of two lower than the yield from ECI films grown near 150–155 K. However, we find that 40 ML of ASW deposited on top of ECI does not crystallize to form PCI, but instead exhibits a D^+ yield characteristic of the buried ECI film, suggesting that nucleation proceeds from the buried interface. These results are relevant to understanding the thermodynamics and crystallization of vapor-deposited ice under various growth conditions.

2. Experiment

The experiments were performed in a UHV chamber (base pressure 2×10^{-10} Torr) equipped with a pulsed low-energy electron gun, a quadrupole mass spectrometer (QMS), and a time-of-flight (TOF) spectrometer with unit mass resolution. The electron beam has a typical current density of 10^{14} (electrons/cm²)/s (continuous beam), and a beam spot size of ~ 1.5 mm. The electron beam was pulsed at 200 Hz, with a pulse width of 700 ns, giving an effective electron dose of about 10^{10} (electrons/cm²)/s. The incident electron energy was 100 eV. The Pt(111) substrate was mounted in thermal contact with a liquid-nitrogen reservoir, and was radiatively heated by a tungsten filament. The substrate temperature was monitored with a thermocouple spot-welded to the substrate and a computer-controlled feedback system drove the temperature ramp at a rate of 8 K/min.

Ice coverages are reported in monolayers of ice, where 1 ML is defined as the number of water molecules in a complete bilayer of the (111) face of cubic ice. The samples were prepared by depositing 40 ML films of D_2O ice at a rate of 4–8 ML/min, with the film thickness calibrated by comparing TPD spectra with previously published results [4,5]. D_2O was used to discriminate against signal from background H_2O. P-ASW samples were deposited at 90 K, and ECI samples were deposited between 150 and 155 K. Following deposition, the samples were annealed at their respective growth temperatures until the background D_2O pressure fell below 10^{-9} Torr (2–3 min), and were then cooled to 90 K prior to beginning the measurements. The ASW–ECI multilayer sample was prepared by depositing 40 ML of ECI at 150 K, cooling, and depositing a further 40 ML at 90 K. The desorption rate of crystalline ice is not negligible above 150 K [8]. As a consequence, the crystalline films examined here may be somewhat thinner than 40 ML.

A negative 75 V extraction pulse was applied to the TOF grid following the incident electron pulse to ensure collection of all cations. The primary cation observed was D^+, with a small H^+ signal due to trace amounts of H_2O and HDO in the ice

film. The H$^+$ TOF peak was well separated from the D$^+$ peak, and does not contribute to any of the reported data. The total D$^+$ yield was measured by integrating the area under the TOF peak as a function of sample temperature.

3. Results and discussion

Fig. 1 shows the ESD yield of D$^+$ from P-ASW and ECI samples as a function of temperature from 90 to 190 K. The data from the P-ASW was acquired with a 90→130→90→190 K (A→B→C→D) temperature cycle. The irreversible increase in yield as the P-ASW film is heated from 90→130→90 K (A→B→C) is related to the collapse of pores and the formation of normal ASW [17], and is observed only on P-ASW films, not on normal ASW or crystalline ice. Following pore collapse, the yields of both ASW and ECI samples are similar, and generally increase monotonically with temperature. At 150 K, the ASW yield begins to decrease, and the steep drop at 155 K is due to the amorphous–crystalline (a–c) phase transition,

where the ASW film converts to PCI. The yield then rises briefly at 165 K, and disappears as the ice film sublimes [16,17]. The relationship between the observed D$^+$ yields and the D$_2$O thermal desorption rate are discussed in Refs. [16,17]. In contrast, the D$^+$ yield from ECI shows no phase transition at 155 K, because the film is already crystalline. Above 155 K, the yield from ECI is larger than the yield from crystallized ASW, and at about 170 K the ECI film also sublimes. These data serve to illustrate two points: P-ASW exhibits a characteristic irreversible increase in yield as the film is heated to 120 K, and the D$^+$ yield from ECI is comparable to or greater than the yield from ASW, until the a–c phase transition. Near 160 K, both films are crystalline, but the yield from ECI is a factor of two larger than the PCI.

Fig. 2 shows the D$^+$ ESD yield from PCI as a function of ice temperature. In this experiment, the PCI film was prepared by annealing a normal (non-porous) ASW film through the a–c phase transition (A→B), and cooling to 90 K (C). The drop in yield due to the a–c phase transition at 155 K is evident. The resulting PCI sample was then heated to sublimation (C→D), showing only
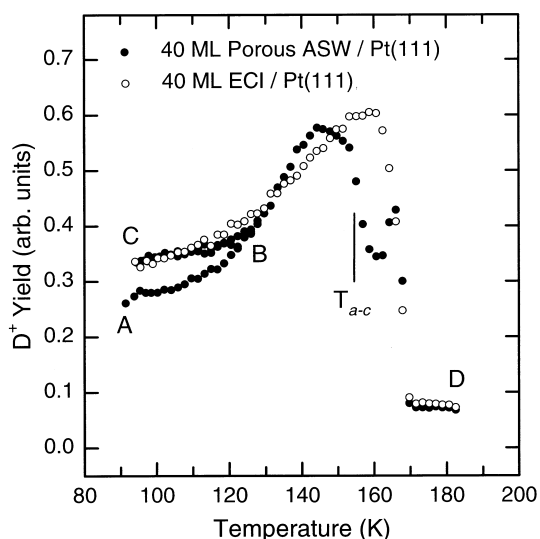

Fig. 1. The temperature dependence of the D$^+$ ESD yield from a 40 ML porous amorphous solid water (P-ASW) film deposited on Pt(111) at 90 K (solid circles) and an epitaxial crystalline ice (ECI) film deposited on Pt(111) between 150 and 155 K (empty circles). Letters identify points of interest described in text. T_{a-c} marks the amorphous–crystalline phase transition.
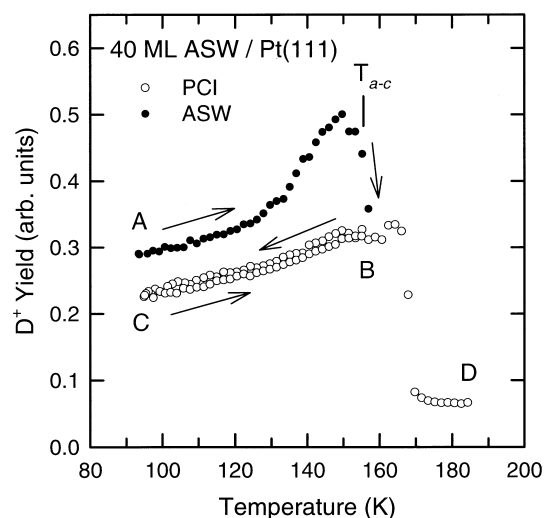
Fig. 2. The temperature dependence of the D$^+$ ESD yield from an ASW film grown at 110 K. The temperature was cycled from 90→155→90→190 K (A→B→C→D). Up until the a–c phase transition, the film is ASW (solid circles). After crystallization (B→C→D), the film is polycrystalline (open circles). Arrows show the direction of the temperature gradient.

a smooth increase in yield with temperature. The yield from PCI is lower than the yield from ASW (and ECI, see Fig. 1) over the entire temperature range examined. The reason for the low yield of PCI relative to ASW and ECI is not known, but may be related to a rougher surface [17], a random sampling of ice facet domains, or perhaps the presence of grain boundaries. A study of the shear modulus of ASW, ECI and PCI films found substantial differences between ECI and PCI, suggesting differences in the long-range order [21].

If we deposit ice at low temperature (90 K) on top of a crystalline film, what form does the overlayer take? If the overlayer is amorphous, does it crystallize to form polycrystalline ice or ECI? To examine these questions, we first deposited 40 ML of ice between 150 and 155 K to form an ECI film. The sample was then cooled to 90 K, and another 40 ML of ice was deposited on top of the ECI layer. Fig. 3 shows the D^+ yield from the resulting multilayer system as the temperature was cycled from $90 \rightarrow 125 \rightarrow 90 \rightarrow 185$ K ($A \rightarrow B \rightarrow C \rightarrow D$). The irreversible increase in yield as the temperature is cycled from $A \rightarrow B \rightarrow C$ is reminiscent

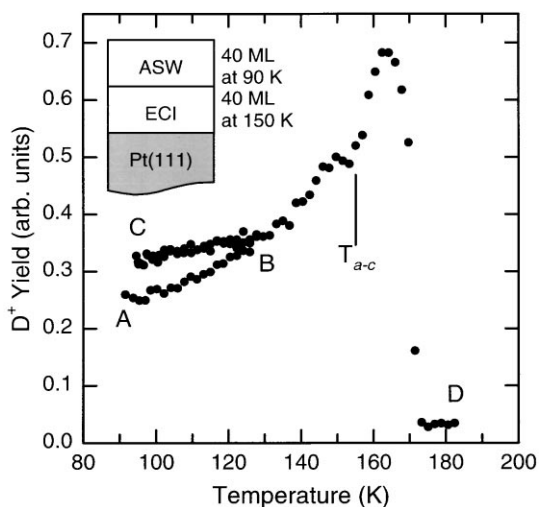Fig. 3. The temperature dependence of the D^+ ESD yield from an ASW–ECI multilayer system. The temperature was cycled from $90 \rightarrow 130 \rightarrow 90 \rightarrow 190$ K. The irreversible increase in yield as the temperature is cycled from $A \rightarrow B \rightarrow C$ strongly suggests that the overlayer is deposited as the P-ASW polymorph. The rise in yield following T_{a-c} suggests that the amorphous overlayer has crystallized to the ECI polymorph.

of the behavior of P-ASW (Fig. 1), suggesting that the overlayer is deposited as the P-ASW polymorph. The crystalline substrate does not appear to have affected the overlayer growth in this case. The sample was then heated from 90 K to sublimation ($C \rightarrow D$). Near 155 K, where we expect to see the yield drop as the ASW film becomes polycrystalline, we observe only a small dip in the yield. Beyond 155 K, the yield rises to a value characteristic of ECI (Fig. 1), rather than PCI. We conclude that the amorphous overlayer has crystallized to ECI, the same form as the buried film. The buried crystalline ice appears to affect strongly the crystallization of the amorphous overlayer. A similar propensity for interface-mediated crystallization of ice has also been observed in a recent thermal desorption study [22].

This behavior can be understood if the thermal energy required to form a crystalline nucleation center in amorphous ice is larger than the energy needed to add water molecules to an existing crystalline interface. In the bulk ASW, nucleation centers need to form by thermal activation before the film can crystallize. There is no preferred axis of symmetry in the amorph, and the random orientation of nucleation centers leads to a polycrystalline film, with a grain size determined by the average distance between centers [23]. At the amorphous–crystalline interface, however, a large nucleation plane is already in existence. The ECI surface acts as a template for the propagation of a 'crystallization front' that moves through the amorphous film, and this results in a surface structure similar to that of the buried ECI film. Our observation that the crystallized ASW–ECI multilayer shows an ECI-like surface structure implies that nucleation and growth from the interface occurs at a lower temperature than the formation and growth of random centers in the amorphous film. This is consistent with the work of Dohnálek et al. [22], which demonstrated that crystallization under similar conditions is limited by the barrier associated with the propagation of the ASW–ECI interface rather than the kinetic barrier associated with the formation of bulk nucleation embryos. The kinetics and energetics of ice crystallization suggest that it is possible to produce a PCI surface if the amorphous overlayer

is thick enough, or if the temperature ramp is sufficiently fast [22].

4. Conclusion

In this paper, we have demonstrated the utility of ESD for monitoring surface and structural phase changes in ice with temperature. We have presented a study in which the amorphous–crystalline phase transition in nanoscale D_2O ice films was monitored by measuring the D^+ ESD yield as a function of temperature. PCI is found to exhibit a lower ESD yield than ECI films, suggesting that the long-range crystalline ordering is different for the two polymorphs. Ice deposited at 90 K on top of ECI yields a porous amorphous overlayer, with no evidence that the crystalline substrate plays a role in the growth. The ice substrate does, however, affect the crystallization of the amorphous overlayer, producing a surface similar to the buried epitaxial film, rather than PCI. These results suggest that crystallization of the amorphous–crystalline multilayer proceeds by nucleation from the buried interface, rather than from random nucleation centers in the amorphous film.

Acknowledgements

References

[1] R.E. Johnson, Rev. Mod. Phys. 68 (1996) 305.
[2] N.J. Sack, R.A. Baragiola, Phys. Rev. B 48 (1993) 9973.
[3] R.S. Smith, C. Huang, B.D. Kay, J. Phys. Chem. 101 (1997) 6123.
[4] R.S. Smith, C. Huang, E.K.L. Wong, B.D. Kay, Surf. Sci. 367 (1996) L13.
[5] R.J. Speedy, P.G. Debenedetti, R.S. Smith, C. Huang, B.D. Kay, J. Chem. Phys. 105 (1996) 240.
[6] P. Löfgren, P. Ahlström, D.V. Chakarov, J. Lausma, B. Kasemo, Surf. Sci. 367 (1996) L19.
[7] M.S. Westley, G.A. Baratta, R.A. Baragiola, J. Chem. Phys. 108 (1998) 3321.
[8] D.E. Brown, S.M. George, C. Huang, E.K.L. Wong, K.B. Rider, R.S. Smith, B.D. Kay, J. Phys. Chem. 100 (1996) 4988.
[9] M.G. Sceats, S.A. Rice, in: F. Franks (Ed.), Water, a Comprehensive Treatise, University of Cambridge, Cambridge, UK, 1982.
[10] E. Mayer, R. Pletzer, Nature 319 (1986) 198.
[11] K.P. Stevenson, G.A. Kimmel, Z. Dohnálek, R.S. Smith, B.D. Kay, Science 283 (1999) 1505.
[12] J. Braun, A. Glebov, A.P. Graham, A. Menzel, J.P. Toennies, Phys. Rev. Lett. 80 (1998) 2638.
[13] N. Materer, U. Starke, A. Barieri, M.A. Van Hove, G.A. Somojai, G.-J. Kroes, C. Minot, Surf. Sci. 381 (1997) 190.
[14] N. Materer, U. Starke, A. Barbieri, M.A. Van Hove, G.A. Somorjai, G.-J. Kroes, C. Minot, J. Phys. Chem. 99 (1995) 6267.
[15] A. Glebov, A.P. Graham, A. Menzel, J.P. Toennies, J. Chem. Phys. 106 (1997) 9382.
[16] M.T. Sieger, W.C. Simpson, T.M. Orlando, Phys. Rev. B 56 (1997) 4925.
[17] M.T. Sieger, T.M. Orlando, Surf. Sci. 390 (1997) 92.
[18] D.E. Ramaker, Chem. Phys. 803 (1983) 18.
[19] W.C. Simpson, M.T. Sieger, T.M. Orlando, L. Parenteau, K. Nagesha, L. Sanche, J. Chem. Phys. 107 (1997) 8668.
[20] W.C. Simpson, T.M. Orlando, L. Parenteau, K. Nagesha, L. Sanche, J. Chem. Phys. 108 (1998) 5027.
[21] J. Hessinger, R.O. Pohl, J. Non-Cryst. Solids 208 (1996) 151.
[22] Z. Dohnálek, R.L. Ciolli, G.A. Kimmel, K.P. Stevenson, R.S. Smith, B.D. Kay, J. Chem. Phys. 110 (1999) 5489.
[23] S. Trakhenberg, R. Naaman, S.R. Cohen, I. Benjamin, J. Phys. Chem. B 101 (1997) 5172.